Materials & Design 212 (2021) 110285

Contents lists available at ScienceDirect

Materials & Design

journal homepage: www.elsevier.com/locate/matdes

Metarpillar: Soft robotic locomotion based on buckling-driven elastomeric metamaterials

B. Grossi [a,*], H. Palza [a,b,*], J.C. Zagal [a,c,*], C. Falcón [a,d], G. During [a,e]

[a] ANID – Millenium Nucleus of Soft Smart Mechanical Metamaterials, Santiago, Chile
[b] Departamento de Ingeniería Química, Biotecnología y Materiales, Facultad de Ciencias Físicas y Matemáticas, Universidad de Chile, Santiago, Chile
[c] Departamento de Ingeniería Mecánica, Facultad de Ciencias Físicas y Matemáticas, Universidad de Chile, Santiago, Chile
[d] Departamento de Física, Facultad de Ciencias Físicas y Matemáticas, Universidad de Chile, Santiago, Chile
[e] Instituto de Física, Pontificia Universidad Católica de Chile, Casilla 306, Santiago, Chile

HIGHLIGHTS

- Buckling-driven elastomeric auxetic modules can be used to design a novel and efficient bioinspired caterpillar soft robot.
- A pneumatic control compressing each module allowed a dynamic-anchoring process mimicking the mechanism of caterpillars.
- Our bio-inspired soft robot based on buckling actuator metamaterial units share dynamic similarity with caterpillars.

GRAPHICAL ABSTRACT

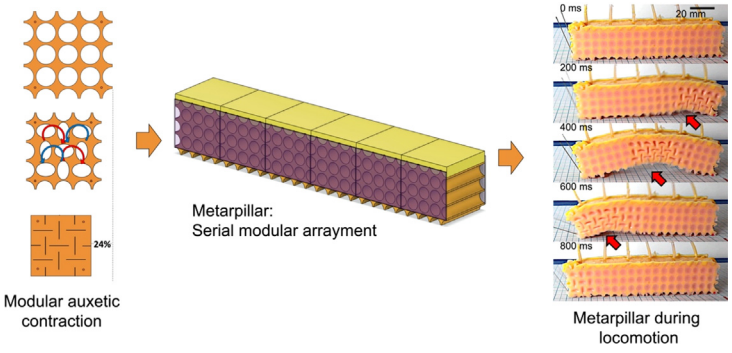

ARTICLE INFO

Article history:
Received 17 August 2021
Revised 15 November 2021
Accepted 24 November 2021
Available online 24 November 2021

Keywords:
Metamaterials
Biomimetic
Soft Robots
Buckling-Driven Units

ABSTRACT

Mechanical instabilities are emerging as novel actuation mechanisms for the design of biomimetic soft robots and smart structures. The present study shows that by coupling buckling-driven elastomeric auxetic modules actuated by a negative air-pressure, a novel metamaterial-based caterpillar can be designed—the Metarpillar. Following a detailed analysis of the caterpillar's locomotion, we were able to mimic both its crawling movement and locomotion by using the unique isometric compression of the modules and properly programing the anterograde modular peristaltic contractions. The bioinspired locomotion of the Metarpillar uses the bending triggered by the buckling-driven module contraction to control the friction through a dynamic anchoring between the soft robot and the surface, which is the main mechanism for locomotion in caterpillars and other crawling organisms. Thus, the Metarpillar not only mimics the locomotion of the caterpillar but also displays dynamic similarity and equivalent, or even faster, speeds. Our approach based on metamaterial buckling actuator units opens up a novel strategy for biomimetic soft robotic locomotion that can be extended beyond caterpillars.

1. Introduction

Animal locomotion is a source of inspiration for the creation of intelligent machines and materials [1–3]. Various animals rely on soft tissues to move in complex unpredictable environments, in turn inspiring the development of soft robotics—a discipline with

* Corresponding authors at: ANID – Millenium Nucleus of Soft Smart Mechanical Metamaterials, Santiago, Chile.
E-mail addresses: b.grossi@uchile.cl (B. Grossi), hpalza@ing.uchile.cl (H. Palza), jczagal@ing.uchile.cl (J.C. Zagal).

https://doi.org/10.1016/j.matdes.2021.110285
0264-1275/

applications in medicine, human assistance, and industry in the present day [3–6]. Due to the complexity of the locomotion problem, the first studies in the field concentrated on the numerical simulation of soft bodies [7]; the research focus then moved to novel fabrication techniques, enabling the production of a broad set of experimental prototypes [8–18]. Recent studies have concentrated on the design of internal material architectures of soft robots, taking advantage of the mechanical properties of intelligent materials while avoiding the use of external complex control systems [3,19–20]. Nowadays, it is recognized that developing a proper bio-inspired robot mimicking a soft-bodied animal's process, such as locomotion, needs the right combination of materials, control mechanisms, and energy sources [3,17].

Mechanical instabilities such as snap-throughs, buckling, wrinkling, and creasing, which were historically regarded as failures to be avoided, are now exploited for the design of new smart structures with specific functionalities. Recent examples include elastomeric baromorphs, programmable mechanical metamaterials, soft swimming robots, and soft-robotic tentacles with three-dimensional mobility [21–27]. Buckling, in particular, is an elastic instability occurring at a critical stress with large displacements, without any relevant addition of stress, and has been recently highlighted as a novel actuation mechanism for soft robots due to the potential for control in the deformation obtained. This instability can be used to produce adaptive structures with controlled shape changes, allowing for the design of responsive and reconfigurable devices [22,28]. For instance, two-dimensional periodic elastomeric porous structures undergo controlled deformation with the critical buckling stress, transforming a square array of circular holes into periodic patterns of alternating orthogonal ellipses through a cooperative torsion and collapse of the beams [28–29]. These geometries and patterns facilitate the design of a family of buckling-driven mechanical metamaterials, thanks to their properties of high level programmability and negative Poisson ratios (auxetic behavior); these properties are useful to program the deformation of the structures [30]. Buckling in elastomeric soft robotic actuators has been explored mainly under negative pressure (vacuum) [31]. The application of negative pressure to a buckling auxetic structure containing elastic beams with interconnected and deformable cavities produces useful motions through bends and buckles [24–25]. Yang et al. proposed these structures as "buckling actuator units" that can be modular and arranged in different configurations, according to the task at hand [24–25]. Therefore, elastomeric porous metamaterials actuated by a negative pressure are ideal units for the design of bioinspired soft robots, taking advantage of the controlled deformation and nonlinear motions of buckling-driven auxetic structures [24–25]. Notably, buckling-driven vacuum actuators are more complex than stretching-driven soft robots actuated by positive pressure [31].

In this context, caterpillars are of particular interest. They are simply shaped animals whose locomotion mechanism is based on pressurizing units of connected soft cylinders that endow caterpillars with the capacity to display large deformations and also climb complex three-dimensional environments with only a few muscle groups [17,32–33]. During locomotion, caterpillars use the substrate to transmit forces from each contact point to other parts of the body. This is biomechanically distinct from most of the soft-bodied terrestrial animals that crawl through stiff hydrostatic structures [32–33]. By controlling the timing and location of this substrate attachment through their legs and prolegs, caterpillars can move forward by crawling, inching, or a combination of both motion modes [18,34–38]. *Manduca sexta* is one of the simplest and most studied caterpillars since it only moves via a crawling motion. Crawling in a caterpillar consists of a broad longitudinal peristaltic contraction wave (anterograde wave), and it moves forward through successive phase delays, presenting a tail-to-head propagation that is the opposite of the head-to-tail contraction wave observed in earthworms (retrograde wave) [33,37–40]. This wave of muscle contraction (peristalsis) serves primarily to reduce the grip between the body and the substrate, and redistribute mechanical energy stored in elastic tissues [15,32,39–40]. This oscillatory dynamic anchoring process with the substrate explains the locomotion of the caterpillar.

Despite the growing interest in design novel bioinspired soft robots, the outstanding behavior of mechanical metamaterials have been barely used in this regard. The relationship between metamaterial architecture and mechanical properties has been mainly used for design complex structures with tailored mechanical performance [41]. For instance, some recent examples focused on design mechanical metamaterials with improved absorption impact and compression resistance [42], and auxeticities [43,44]. Beside these applications, the use of properly designed mechanical metamaterials has been forecasted to produce a paradigm shift in soft robots toward intelligent machines [13,45]. Our study explores this concept focusing on the first design of a bioinspired soft mechanical metamaterial based on an auxetic structure. We show that the contraction of buckling-driven elastomeric metamaterial modules allows the design of a metamaterial-based caterpillar—the Metarpillar. Our approach introduces a novel soft-robotic locomotion mechanism that can be easy extended to other bioinspired systems.

Our design was aimed at producing a soft robot that mimics caterpillar locomotion by controlling the substrate attachment along its body, producing a tail-to-head peristaltic wave of contraction. Accordingly, we designed a set of soft cubic buckling actuators, each displaying a spatially coordinated volume change, inspired by the segmental volume change in caterpillars. Besides having a large internal cavity containing a liquid called hemolymph, the model comprises of segmented external locomotor muscles; each segment not only contains muscles but also tracheae with breathing tubes [15,32,46]. Although the hemolymph is an incompressible liquid moving freely across the body, the tracheae of each muscular segment can be compressed (losing inner air), partly explaining the local muscular contraction of the caterpillar. The muscular contraction increases the internal hydrostatic pressure of caterpillar segments and reduces their volume [15,32,39,47]. The contraction wave along the caterpillar body is responsible for its crawling action via a dynamic anchoring mechanism with the substrate. For these reasons, our bioinspired Metarpillar soft robot requires a set of independent contraction segments, such as those obtained through the buckling actuator unit [24].

Fig. 1a shows the timeframes of a caterpillar (lateral view) during a typical horizontal stride, obtained from the peristaltic anterograde wave (green arrow). The observed segmental peristaltic contraction causes a hump, thereby reducing the contact of the body with the substrate (swing phase). The geometrical changes taking place in each segment can be analyzed by defining three consecutive segments or units near the tail of the caterpillar (see Fig. 1a and b). From this lateral view, the wave contraction shows the morphological and volumetric changes in the segments during crawling. The segments present a rectangular-like shape when relaxed, and this changes to a trapezoid-like geometry when contracted. The morphological changes of these segments comprise three stages: relaxed, semi-contracted, and contracted (Fig. 1b). Fig. 1c shows that the crawling process can be mimicked by using a coordinated contraction wave of three segments that transition from a rectangular to a trapezoidal shape. The simultaneous contraction of the coupled units (three modules in the example of Fig. 1c) produces a dorsal bending in the body that controls the anchoring process with the substrate. Therefore, the caterpillar-bioinspired soft robot has to be constructed using independent

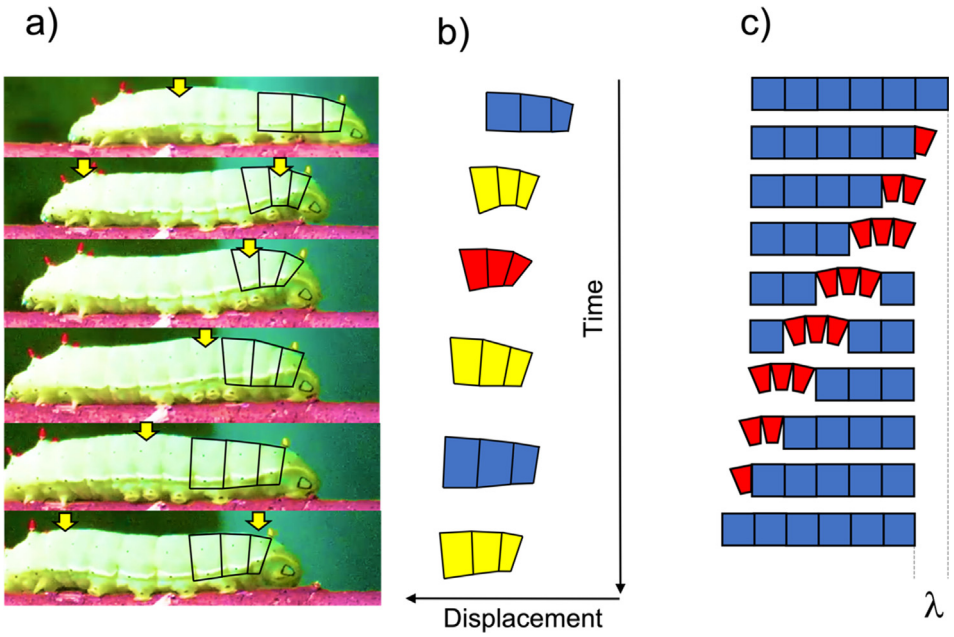

Fig. 1. Schematic representation of the contraction process of real caterpillar during locomotion. (a) A sequence of images (lateral view) taken during a complete forward stride of a caterpillar (*Manduca sexta*). Caterpillars can be designed as composed of independent segments able to contract, and the boundary of three of the last body segments is marked with black lines. The green arrows show the hump where the peristaltic contraction occurs, which moves from back to front. (b) A schematic representation of the contraction process of the segment, assuming that the segments change from a rectangular-like to a trapezoid-like form. The blue color depicts a relaxed segment, the yellow a semi-contracted segment, and the red a contracted segment. (c) Diagram of a functional model of a six modules caterpillar during a "3 modules" locomotion pattern. The blue color represents the relax modules (rectangular-like) and the red color the contracted modules (trapezoid-like). λ corresponds to the length traveled by each locomotor cycle. The process shown in c) represents a gait cycle for a "3 modules" peristaltic contraction for the locomotor pattern. The peristaltic contraction produces a dorsal-bending in the soft-robot that replicates the contraction wave of the caterpillar. (For interpretation of the references to color in this figure legend, the reader is referred to the web version of this article.)

controlled units, each accounting for a precise volume reduction during the shape change from rectangular to trapezoidal. By controlling the time and position of the contractions (and the dorsal-bending), the locomotion pattern of the caterpillar can be mimicked. These characteristics can be achieved by adding a dorsal reinforcement on the buckling-driven metamaterial actuator unit, with a programmable vacuum actuation system reproducing the dynamic of Fig. 1c.

2. Materials and methods

For the main body of the soft robot (module segments), a commercial silicon elastomer was used (Zhermack, Elite Double 16, http://www.zhermack.com) with a Shore hardness of 16. A stiffer silicone (Zhermack, Elite Double 32, zhermack) with a Shore hardness of 32 was further used at the upper part of the soft robots, and a more flexible silicone with a hardness shore of 8 was used to create the lateral faces of the robot. All these liquid silicones were cured at room temperature for 40 minutess to obtain the high elastic solid silicone. Fig. 2 shows the use of each silicone elastomer.

Our robotic caterpillar's (Metarpillar) design involves a modular approach in which soft actuating units are arranged in a series, similar to the body segments in the anatomy of caterpillars. We focused on producing modular body segments using buckling actuator units that reproduce the rectangular-to-trapezoidal deformation of a caterpillar's body segments during locomotion. The aim was to reproduce the lateral deformation of the segments without paying attention to deformations that can be observed from above or below the caterpillar. With this in mind, we established the following design requirements for the modules: (1) an unactuated initial rectangular shape with (2) a rapid expansion/contraction into an actuated trapezoidal shape wherein (3) the lower part gets contracted and the upper part extended.

The majority of soft robotic machines have been implemented using soft pneumatic actuators under positive pressure, consisting of networks of microchannels connecting hollow chambers. Increased pneumatic or fluidic pressure produces expansion of chambers, resulting in different types of deformation such as bending and curling. Deformation is primarily governed by the outside chamber architecture and materials selected for the exterior walls. In fact, some design principles have been reported previously. However, instead of following the predominant approach, we explored the use of buckling-driven elastomeric metamaterials for governing the actuation of soft units under negative pressure. Besides the abovementioned reversible-nonlinear behavior, these systems present practical advantages related to safety and lifetime. These are safer than positive pressure systems that can explode when subjected to overpressure or when the material suffers ruptures due to fatigue. The strain of these negative-pressured systems is limited during actuation; therefore, the lifetime of these systems should be higher than systems governed by positive pressure.

The choice of buckling-driven metamaterial units imposes the challenge of focusing the design on the internal architecture of the material used for the fabrication of actuators. We conceived each unit as a vacuum-controlled buckling actuator, whose deformations were constructed to mimic the rectangular-to-trapezoidal deformation observed in caterpillar segments. The actuator, shown in 2, is composed of two parts, where the lower part has the shape of a cube and contains a pattern of parallel circular deflation chambers. The chambers are disposed in a direction orthogonal to the main axis of the caterpillar body and parallel to the ground. The upper part is a stiff dorsal non-buckling layer that's added at the top of the cube to prevent contraction of the upper part of the actuator. Each cube is covered by a one-millimeter thin membrane of

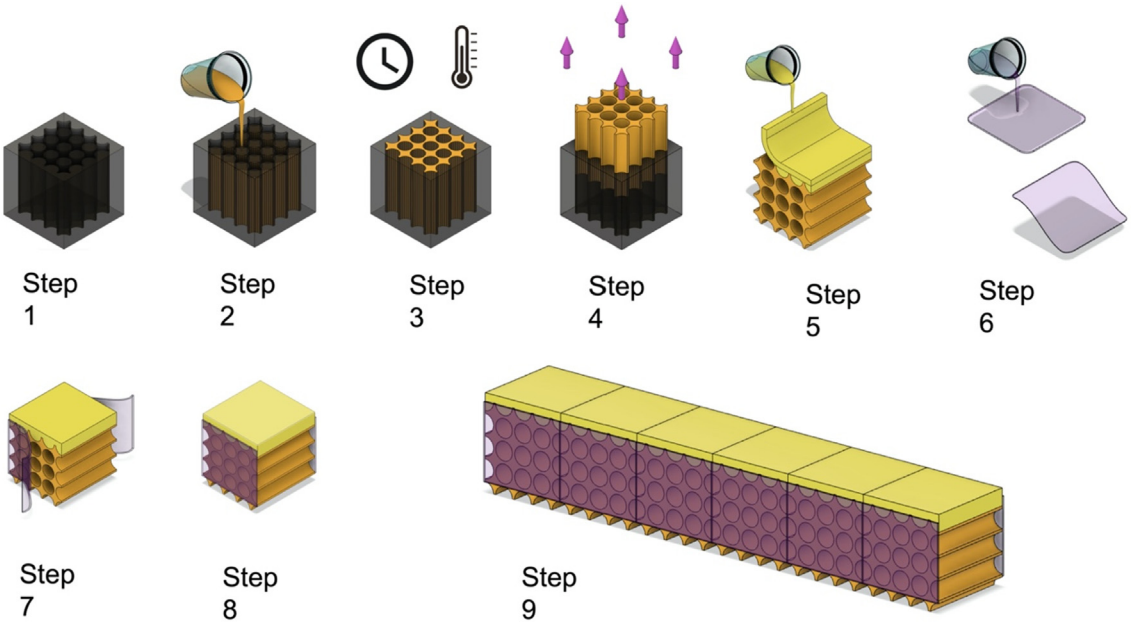

Fig. 2. Design and construction of soft cubic buckling actuators and the resulting caterpillar robot. Step 1, 3D printed molds are fabricated for the lower and upper parts. Step 2, liquid silicone of shore 16 is cast on each mold. Step 3, molds are cured at room temperature for 40 min. Step 4, silicone parts are extracted from the molds. Step 5, the upper layer is glued back-to-back using liquid silicone of shore 32. Step 6, a thin one-millimeter membrane of silicone of shore 8 is produced by spin coating liquid silicone. Step 7, this layer is then glued to the lateral faces of the cube. Step 8, a thin silicone tube was introduced on the top part of each module. The deflation chambers are all connected to this silicone tube using an internal cut serving as a pneumatic link between cavities. Step 9, the entire robot is assembled by gluing together the modules in an arrangement of six modules.

silicone that isolates the circular deflation chambers from the exterior.

Fig. 2 shows the different steps used to design the buckling actuators together with the fabrication process of the entire robot. Each part was produced using soft lithography [48]. The fabrication process consisted of nine steps: First, 3D printed molds were fabricated for the lower and upper parts. Then, liquid silicone was cast on each mold. Third, the molds were cured at 20 °C for 40 min. In Step 4, the silicone parts were extracted from the molds. Subsequently, the upper layer was glued back-to-back using liquid silicone. In Step 6, a thin one-millimeter membrane of silicone was produced by spin coating from liquid silicone. Following this, in Step 7, this layer was then glued to the lateral faces of the cube. Then, a thin silicone tube was introduced on the top part of each module. The deflation chambers were all connected to this silicone tube, thanks to an internal cut serving as a pneumatic link between cavities. Finally, in Step 9, the entire robot was assembled by gluing together the modules in an arrangement of six modules. The final construction stage consisted of 3D printing a test surface with a directional anisotropic pattern (one-direction toothed surface) that promotes displacement in the forward direction (Fig. 7, c) and attaching a pair of rigid tips to each end of the Metarpillar (Fig. 7, d). These tips served to increase friction and establish secure anchoring points with respect to the horizontal surface used for the locomotion test. Each module was then connected to a flexible tube which was connected to a pressurized airline. The air entering each module was controlled using an on–off switching solenoid valve (12-V/4-psi generic) having a microcontroller unit (i.e. Arduino UNO system). Although the solenoids that control the air flow of each module are an essential component in the locomotor control of our Metarpillar, the on–off switching valve used in our case has a characteristic actuation time of around 15 ms of aperture, that is typical values for these devices. This time is negligible in relation to actuation period of the module contraction of Metarpillar, and therefore the characteristics of the solenoids do not modify the locomotor pattern.

3. Results

3.1. Buckling-drive module

The Metarpillar uses buckling-driven elastomeric metamaterial actuator units made of a two-dimensional periodic array of circular holes with the capacity to be transformed into periodic orthogonal ellipses when actuated [29]. With respect to the design, this structure presents an isomorphic/isometric transformation under compression due to its auxetic properties. To validate this design, we first explored the shape-changing behavior of four buckling modules, all having different geometries under compression (by applying a negative pressure). Fig. 3 shows the elastomeric modules studied: two single modules having either a rectangular or a circular chamber in the center (Fig. 3a and b, respectively) and periodic modules having a 3×3 pattern of chambers with both geometries (Fig. 3c and d for rectangular and circular chambers, respectively). Each module has the same silicon volume (4.9 ml) and internal empty volume (4.9 ml), resulting in a ratio between empty volume and total volume of 0.5.

Interestingly, our buckling-driven metamaterial module, displayed in Fig. 3d, shows isomorphic deformation, meaning that it contracts while preserving its overall aspect ratio. We exploited this feature for controlling the final compression shape of the module by adding constraints in the upper part of the structure to better mimic the morphological changes in a caterpillar's segments.

We investigated the isometric/isomorphic behavior of each module during contraction by tracking the displacement of the eight peripheric key points (black-points in Fig. 2a–d) when actuated. The isomorphic degree of the modules was defined by the geometric similarity ratio (GSR) before and after the actuation. For each key point i of the perimeter ($i = \{1, \cdots, 8\}$)we defined its initial (unactuated) position at points ($p_0^i p_0^i$) and its final (actuated) position at points (p_1^i), with each point defined by its Cartesian coordinates, $p_0^i = (x_t^i, y_t^i)$. We also defined the displacement vector

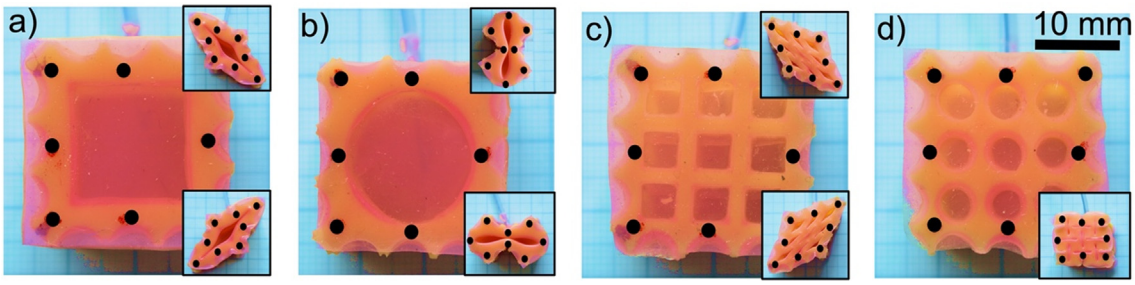

Fig. 3. Pictures of modules implemented with different internal architecture and patterns. (a) Squared chamber, (b) Circular chamber, (c) Squared pattern, and (d) Circular pattern. Figure insets also show different final actuated states after compression, obtained on each module. Each module presents 8 marks (red points) used for the quantification of the isometric compression (geometric similarity ratio or GSR). (see Supplementary Material for details). (For interpretation of the references to color in this figure legend, the reader is referred to the web version of this article.)

$d^i = p_t^i - p_0^i$of each key point, where $\|d^i\|$ is the Euclidean distance between the unactuated and actuated positions of each point *i*. The isometry can be quantified by comparing these d^i with the displacement vectors expected for an ideal isomorphic compression (d_{iso}^i), where the geometry similarity ratio is defined by Eq. (1).

$$GSR = \frac{\sum_{n=i}\|d^i - d_{iso}^i\|}{\sum_{n=i}\|d_{iso}^i\|} \quad (1)$$

The lower the GSR, the greater the degree of isometry. The ideal isomorphic displacement vector d_{iso}^i can be decomposed on a global translation of the module, a global rotation of the module, and an affine compression of the module. By setting the origin of the Cartesian coordinates, such that $\sum_{n=i} p_0^i = (0,0)$, the global translation and rotation were expected to be small and, therefore, neglected for the sake of simplicity. Therefore, the displacement of ideal isomorphic compression can be reduced to a pure affine compression, approximated by Eq. (2).

$$d_{iso}^i = -\frac{1}{2}\frac{v_{extracted}}{v_{initial}} p_0^i \quad (2)$$

where $v_{extracted}$ and $v_{initial}$ are the internal volumes of the modules. We observed that the GSRs were 4.50 for the squared chamber, 11.63 for the circular chamber, 5.16 for the squared pattern, and 0.23 for the circular pattern (metamaterial), meaning that the metamaterial presented the lowest value and, therefore, an almost pure isomorphic compression process. This was due to the buckling of the final geometry of each module. The compression produced shear deformations (as the least energetic mode) in the squared and patterned squared modules and a central collapse via buckling in the circular chamber; all these processes produce a dramatic change in the shape of the modules. Notably, in the circular patterned metamaterial chamber, the compression produced a periodic pattern of alternating orthogonal ellipses under buckling that barely affected the global geometry of the module (Fig. 3d). In consequence, the isometry of the metamaterial module is 20 times larger than the other modules. Another relevant characteristic of the metamaterial is the reproducibility of the final shape; in the square structures and the single circular chamber, two compressed final shapes are produced randomly (see inserts in Fig. 3), while in the metamaterial, only one compressed shape is produced.

The isomorphic compression in the metamaterial module is also characterized by a 24% decrease in the external perimeter when actuated, as opposed to a negligible reduction in the other modules (Fig. 4a). The auxeticity of the module is a remarkable characteristic of our soft robot design; the metamaterial arrangement under compression suffered an isometric size reduction that can be used to program the final shape of the module. As previously explained, during caterpillar locomotion, specific segments undergo a shape change from a rectangular to a trapezoid-like structure (Fig. 4b). This is replicated in our Metarpillar through the addition of a stiff silicon layer on the top-side of the module (Fig. 4c). This layer adds a restriction for isomorphic deformations, which produces a trapezoidal compressed structure that mimics the muscular contractions of a caterpillar (Fig. 4d). The asymmetrical compression is due to segments of the module with a complete buckled state (lower part) that coexist with segments (upper part) with a less-buckled state due to the stiff layer on the top.

Fig. 5 shows the relationship between the negative pressure used to compress the module and the extracted volume resulting from each one of the patterns studied. The pressure was measured using Panasonic Pressure Sensors PS-A, with a sensitivity of 41.6 Pa/mV. The extracted volume was measured using a syringe pump (KDS Legato 111) set at a 9.8 ml/min flow rate, and images and videos of the set were taken with a digital camera, Canon Rebel T6iat, at 30 fps. The area under each curve represents the work needed for each compression cycle. The curves are linear with a slope dependent on the arrangement (single or patterned) rather than the chamber's internal structure and a larger slope for patterned modules. Structure becomes relevant as buckling instabilities develop, which prompts the patterned modules' drastic change from the linear dependence described above. After buckling occurs, the mechanical response display roughly plateaus for a large range of extracted volumes, meaning that a large volume of air can be extracted without any relevant increase in pressure. For instance, the individual circular chamber presents buckling at a much lower volume extracted than the squared chamber, therefore requiring less work. This difference is even more relevant for the patterned chambers, where the circular arrangement (Fig. 4d) buckles and causes structural collapse at a much lower buckling pressure than the squared-patterned chamber. Therefore, the alternating orthogonal buckling collapse of the circular arrangement stores less elastic energy in the bulk of the material [29], thereby providing a more efficient system for compression using negative pressure and, thus, requiring lesser work for the same amount of deformation. After buckling, the circular pattern (red curve) displays a large volumetric change from 1300 to 4000 μL (55% reduction of the original volume) with just small variations in pressure (−2 kPa). Moreover, by analyzing the elastic hysteresis loop, it can be concluded that only a small amount of energy is dissipated in all the modules due to material internal friction. The amount of preserved energy is higher than 92% for all modules, and it is consistent with the elastomeric characteristics of the polymer matrix used.

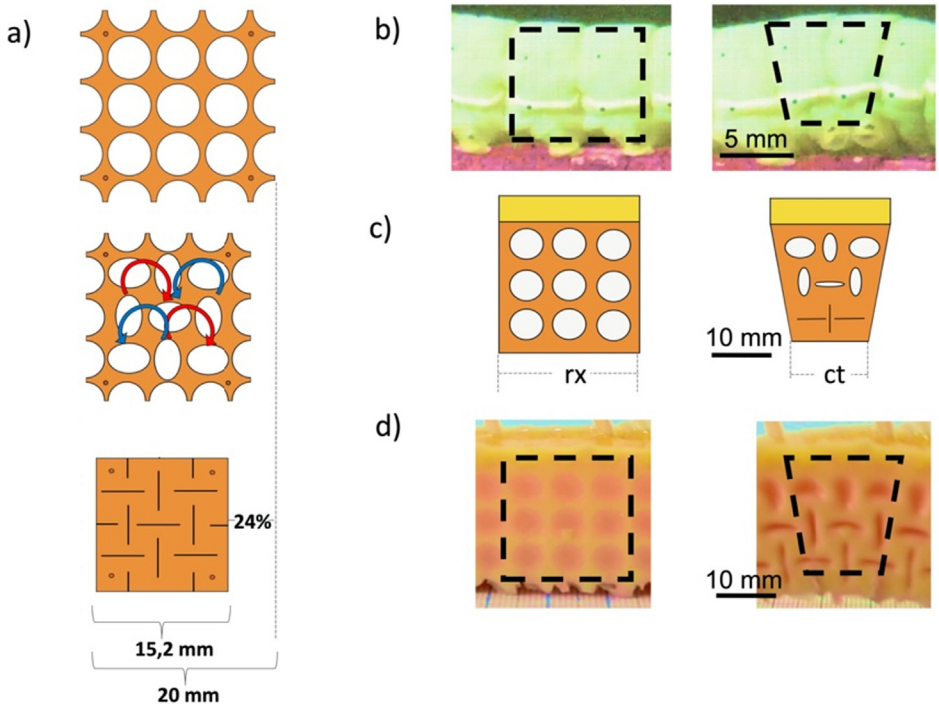

Fig. 4. Representation of a buckling-actuator units. (a) Buckling contraction model of the auxetic metamaterial module showing that during compression, the silicone between the circular holes twist in different directions (red arrows clockwise, and blue arrows anti-clockwise). After the buckling, the maximum linear contraction is 24% of the initial length. (b) Contraction of a caterpillar segment (*Manduca sexta*) showing the change from a square-like to a trapezoid-like shape. (c) Expected contraction model for a module with a stiff silicon on the top-side (yellow). (d) A picture of a buckling-driven module confirming the expected behavior. (For interpretation of the references to color in this figure legend, the reader is referred to the web version of this article.)

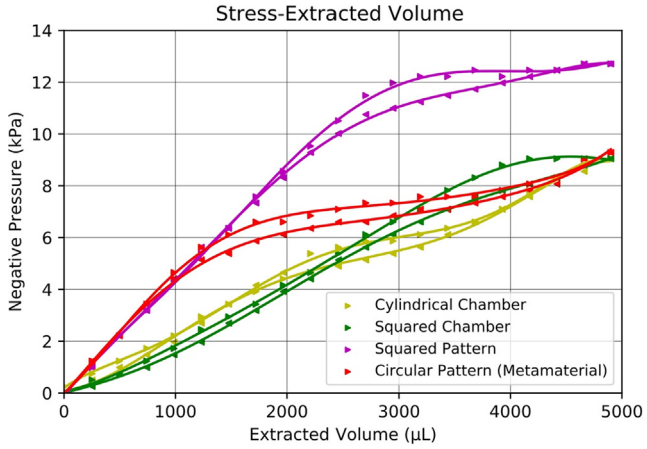

Fig. 5. Relation between negative pressure versus extracted volume for different modules. The case of circular and squared hollow chamber is compared with the case of circular- and squared-patterns. Arrows pointing to the right represent air extraction, while arrows pointing to the left represent natural recovery of the module. Five replicates were made with each module, and the standard deviation was less than 0.3 kPa for all data.

3.2. Buckling-drive locomotion

After the characterization of the individual modules, we analyzed the linear contraction of the Metarpillar, which consists of six buckling-driven metamaterial circular pattern modules in a serial arrangement (Fig. 2) with each module having a layer of reinforcing silicone added to the top (Figs. 2 and 4c). With this structure, we replicated the crawling kinematics of the caterpillar (Fig. 1c) through different configurations of the anterograde (posterior-anterior) peristaltic contractions of the modules by simultaneously applying a negative pressure to a defined number of modules. A specific combination of these peristaltic contractions (defined by the number of modules coupled to compress at the same time) and their propagation through the Metarpillar are defined as the "locomotor pattern", as shown in Fig. 1c, for the "three modules" peristaltic contractions for the locomotor pattern. In "one module" peristaltic contractions, the locomotor pattern starts from the last module because the peristaltic propagation is anterograde; that module relaxes after a time of contraction called "actuator period," and the penultimate module (next module) starts to contract during the same actuator period. The same pattern is repeated with the next modules, generating a peristaltic wave of contraction that involves just one module at the time and finishing when the first module is contracted and relaxed. During "two modules" peristaltic contractions, the locomotor pattern starts contracting only the last module, but after the actuator period of contraction, the module stays contracted while the penultimate module starts to contract during the actuator period. After this two-actuator period, the last module relaxes while the antepenultimate starts to contract during the same actuator period, and this pattern is repeated until the contraction/relaxing process reaches the first module. The same pattern can be extrapolated for three (Fig. 1c), four, five, or six modules of locomotor patterns. We define the gait cycle as the sequence of movements during locomotion, starting with the contraction of the posterior module and finishing when the same module starts to contract again.

We can understand the mechanics of the Metarpillar's locomotion by analyzing its speed, which is defined as the distance (λ) traveled by the six modules in each gait cycle divided by the duration of each cycle (Fig. 1c). This distance (anterograde advance) is associated with the total displacement produced by the peristaltic contraction occurring in individual modules until the total number of modules is actuated, completing a cycle (first three contractions

defined λ in the example of Fig. 1c for the "three modules" locomotor pattern). This contraction defines the anterograde advancement of the Metarpillar, if we assume a perfect anchoring point of the last module after contraction, pushing the other modules when relaxed and generating an anterograde advance. During the next peristaltic contraction (meaning the relaxation of the last contracted module and the contraction of the corresponding module, according to the locomotor pattern, simultaneously), there is no retrograde advancement due to the compensation of these two processes, summing zero displacement. The speed V, equation (3), is λ divided by the actuator period (AP), multiplied by the number of coupled modules defined in the specific locomotor pattern (N), plus six (the total number of modules in the Metarpillar), corresponding to the total time of a gait cycle. Thus, the velocity of locomotion function increases with the number of modules coupled in the locomotor pattern (increasing λ) and decreases with the time of the gait cycle.

$$V = \frac{\lambda}{AP(N+6)} \tag{3}$$

Theoretical speed (TS) of Metarpillar can be computed by equation (3) assuming that λ is always 24% (Fig. 4a), without being affected by the specific locomotor pattern or the actuation period. However, the effect of the actuation period on the effective experimental contraction, under a different locomotion pattern, should be analyzed. Fig. 6a shows that the experimental percentage of the total lineal contraction (experimental λ) of the Metarpillar (with the first module anchored to prevent displacement and avoid surface effects) under different actuation periods is highly dependent on the locomotor pattern and the actuator period. Indeed,

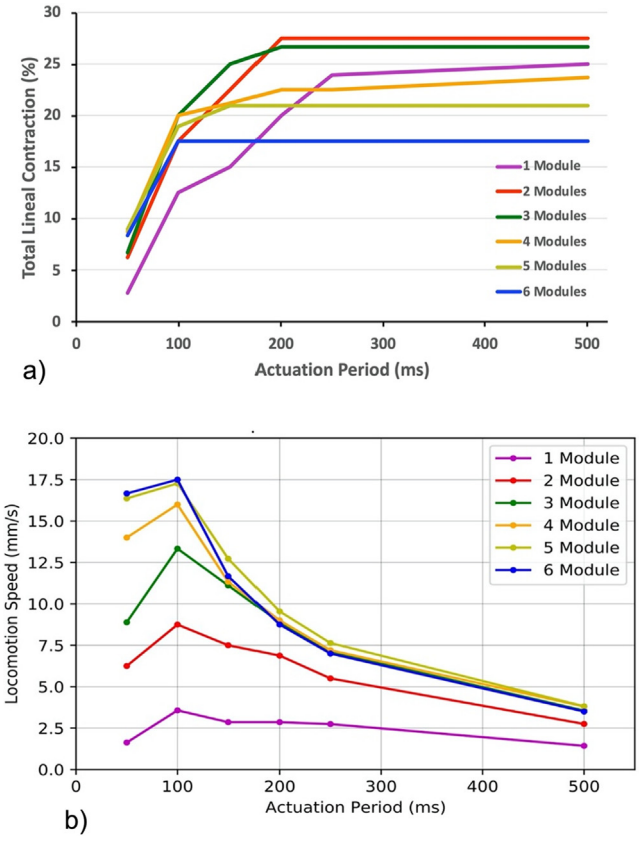

Fig. 6. Behavior of the Metarpillar regarding to actuation period. (a) Experimental contraction of different number of modules with respect to a period of air extraction time. (b) Corrected theoretical speed measured for different actuation periods on the Metarpillar. Curves are shown for varying number of modules.

there is an asymptotic tendency regarding the contraction and actuation period, independent of the locomotor pattern, providing the optimal scenario to maximize the speed of locomotion. With these experimental values of contraction, the corrected theoretical speed was measured through Eq. (3), as displayed in Fig. 6b. The data shows that, independent of the locomotor pattern, there is a specific actuation period optimizing the speed of locomotion, i.e., 100 ms, selected for the locomotor experiments.

After defining the compression time and the speed based on either theoretical or corrected contractions, we focused on replicating the kinematic locomotion of the *Manduca sexta*, as displayed in Fig. 7a, for the specific case of peristaltic contraction locomotor patterns involving "two modules." Fig. 7a confirms that, rather than a simple linear sum of horizontal contractions, the Metarpillar displayed a peristaltic wave as a consequence of the dorsal bending from the buckling-driven module contraction, similar to the caterpillar's wave contraction. Indeed, by observing the complete gait cycle of this locomotor pattern (Fig. 7b), we can see that the crawling locomotion is mimicked as the contraction wave can reproduce the dynamic anchoring of the caterpillar. The crawling was also observed under all locomotor patterns. Therefore, the propagation of the peristaltic contraction forms a contraction wave (dorsal bending) that replicates the crawling and can produce effective horizontal displacement. Notably, this locomotion strategy is attainable on a smooth surface, and without any aids to increase grip, stressing the flexibility of our mechanism and locomotor potential of the peristaltic contraction of anchor waves.

Following confirmation that the Metarpillar was able to translate mimicking a caterpillar, the real speed of locomotion was measured under three different conditions: (i) a flat paper surface and a Metarpillar without any anchors, (ii) a unidirectional toothed surface that promotes unidirectional displacement and a Metarpillar without any anchors (Fig. 7c), and (iii) a unidirectional toothed surface and a Metarpillar with anchors at the ends to reduce sliding (Fig. 7d) (see, Supplementary Materials for details). On a flat surface, the Metarpillar is able to present locomotion with a low speed that is barely independent of the number of modules compressed. On the other hand, using an anisotropic surface, higher speeds can be reached; by further adding anchors, the speed is similar to the corrected theoretical values. When comparing the different speeds achieved with respect to the different locomotor patterns, we observed that the robot increased its speed as more modules were compressed simultaneously, with the exception of using an isotropic surface (Fig. 8).

4. Discussion

4.1. Metamaterial module

It was recently claimed that exploiting metamaterials in advanced soft robots can lead to paradigm shifts in the design, manufacture, and perception of future intelligent machines [13]. Our biomimetic Metarpillar not only contributes to this paradigm shift but also to answering one of the key questions regarding the future impact of soft robotics research: "Why soft?" [49]. The Metarpillar is the first soft robot that uses the isomorphic contraction of buckling-driven metamaterial modules for the design of bioinspired locomotion. This isometric compression, triggered by an elastic instability, is the basic unit for programming the deformation of our modules mimicking the contraction of the caterpillar, for instance, through the addition of a stiff dorsal silicone surface. Following previous reports oriented towards designing soft robots without hard internal/external structures, and fabricated entirely in soft-compliant polymers, our Metarpillar only uses commercial elastomeric polymers and a vacuum-actuated

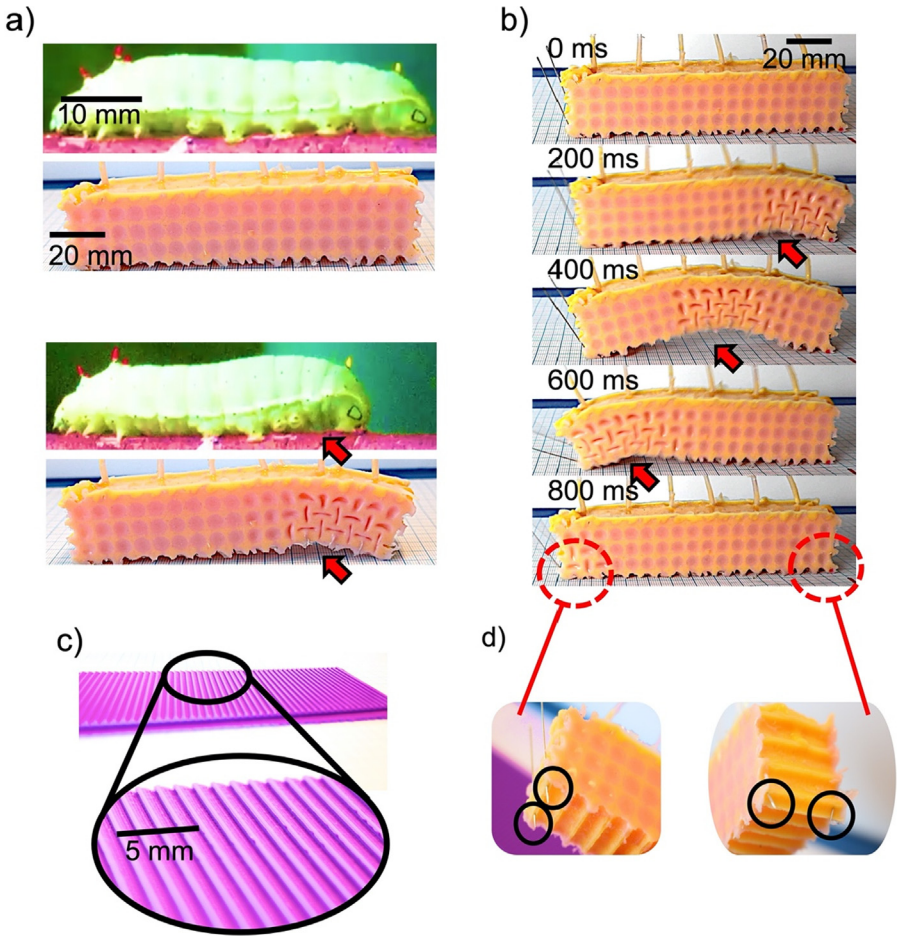

Fig. 7. Biomimetic locomotion of the Metarpillar. (a) Comparison between the locomotion of the caterpillar *Manduca sexta* and the Metarpillar during a "two modules" locomotor pattern. (b) Pictures from the sequence actuation taken during one locomotor cycle of the Metarpillar, with an actuation period of 100 ms with "two modules" locomotor pattern on an isotropic friction surface (paper). Pictures show that actuated buckled modules states coexist with relaxed states due to modules has independent air flow control systems. (c) Frictional anisotropic surface for Metarpillar locomotion. (d) Rigid tips at each end of the Metarpillar mimicking legs and prolegs of the caterpillars to increase grip. Red arrows show the point of anchoring of the peristaltic locomotion based on dynamic anchoring (see, Supplementary Materials for details). (For interpretation of the references to color in this figure legend, the reader is referred to the web version of this article.)

pneumatic structure, showing high efficiencies for mechanical deformation [24–25]. Moreover, it belongs to a new family of soft robots that harvest snap-through instabilities, taking advantage of the nonlinear response [24–25,29,50]. Single-unit buckling actuators were first reported as taking advantage of this instability to program the rotation of a compressed sample [24]. Additionally, more complex actuations, such as locomotion, were obtained by connecting multiple buckling actuators under asymmetric friction. The Metarpillar is a contribution in this context of using a linear configuration of buckling-driven metamaterial modules to mimic a more complex locomotion associated with the crawling of the caterpillar. Notably, our approach can be extended to other bioinspired soft robots, opening up a novel programming tool for other metamaterial locomotive machines.

The Metarpillar design was made possible by considering one of the main advantages of mechanical metamaterial modules: semi-isometric contraction. This outstanding behavior has barely been discussed and applied, despite its high potential impact for the design of actuators and soft robots. We quantified this property by means of the GSR and obtained a value of 0.23 for the metamaterial module, which is much lower than the other module patterns, as expected, due to the internal bending capable of closing the circular holes in a specific pattern. (Fig. 4a) [24,25,27,29,50-52]. This type of contraction is essential not only to build our Metarpillar but also any modular soft robots requiring controlled contractions (e.g., antero-posterior and dorso-ventral). Another relevant result is related to the configuration stability. Current elastic buckling instabilities can jump to a set of different final configurations [28,50], as observed in the squared structures and the single circular chamber, showing bistability and, therefore, two random final shapes (see inserts in Fig. 3). This random post-buckling behavior arises from the asymmetric bifurcation response, preventing its application in actuators and energy harvesting [53]. However, our metamaterial module presented a robust pattern switch with only one compressed final shape [50,54]. Further, the buckling of the beam-like ligaments triggered a sudden transformation of the holes into a periodic pattern of alternating and mutually orthogonal ellipses, explaining the homogeneous and reversible pattern transformation observed in these metamaterial structures. This strong coupling of the square geometry forced a simple bifurcation, thereby explaining the configurational stability [50,54].

The buckling-driven auxetic compression of our modules is characterized by a stress–strain curve having a linear region where the deformation occurs through foreshortening of interstitial vertical ligaments in the structure [24–25,27,54]. At some critical point, the buckling of the ligaments occurs, triggering a plateau in the stress–strain curve where the total stress became independent of

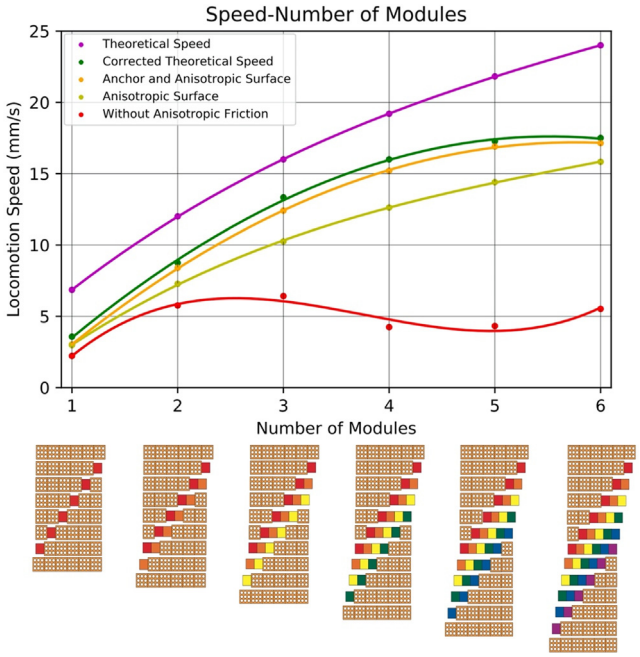

Fig. 8. Locomotion speed as function of the number of modules. Different curves are shown for the case of theoretical speed, corrected theoretical speed, without anisotropic friction, with anisotropic friction and for the case of anchoring protrusions. All these speeds were calculated and recorded with a contraction period of 100 ms.

strain (Fig. 5). This behavior is typically expected for cellular structures under compression but due to the elastomeric nature of the polymer used and the specific configuration of the module in the present design, it is highly reversible and repeatable. This reversible plateau originates from the elastic buckling instability, opening up energetic benefits for actuators [53]. In particular, our module can be deformed by 55% of its internal volume with a pressure differential of only −2kPa (Fig. 5). This result indicates that this highly elastic buckling-driven metamaterial has excellent potential as a mechanical actuator, since a reduced amount of energy is required compared with other topological module configurations. Moreover, the hysteresis in the stress–strain curve indicates that more than 92% of the elastic energy stored during contraction is recovered, meaning that the material is hyperelastic [55], which aligns with what was expected for the polymer used. Highly elastic elements of nature, such as the tendon of a kangaroo or a wallabi, have an elastic energy recovery of around 93% during locomotion [56]. These findings show that our designed module is highly efficient and useful for the creation of soft robots for bio-inspired locomotion. Similar results were found in vacuum-actuated muscle-inspired pneumatic structures (VAMPs), which show thermodynamic efficiency with low loss of energy due to small hysteresis [25]. Other advantages of the buckling-actuator units are the nonlinear motion, low cost, and low density of the components [24,25,27].

4.2. Metarpillar locomotion

Although other locomotion models for buckling based soft robots have been proposed (27), for example in a finite element based method using the rotation of two wheels that are attached through leg-like embedments to the buckling module, our Metarpillar exploits the deformation of the their body. Our results show that by coupling six metamaterial-based modules in a linear configuration with a stiff dorsal silicone surface, biomimetic crawling can be facilitated through the compression and associated bending of the modules. This crawling is a complex process as it depends on several variables besides the pure contraction of each module. For instance, the theoretical speed (from Equation (3), assuming a contraction of 24% for each module) displayed in Fig. 8 shows the relevance of the locomotion pattern (i.e., number of simultaneous modules compressed) with increasing asymptotic behavior as the number of coupled modules increases (Fig. 8). This tendency arises from the nature of Equation (3), where λ is divided by the actuator period times the number of coupled modules (N) plus six (total number of modules). Since λ also depends on the number of contracted modules, the resulting function (proportional to N/N + 6) behaves asymptotically for a specific actuator period (Fig. 8). This theoretical speed assumes that the contraction of the isolated module is replicated in the six serial modules as well as a perfect unidirectional anchor for a no-retrograde slip (ideal anisotropic friction). However, as concluded recently by numerical models, the actuation of buckling-driven locomotion robots triggered by a negative pressure is highly dependent on the dynamic of the pressure applied with a high non-linear relationship with the effective displacement (27). Indeed, by comparing this theoretical speed with the corrected theoretical velocities displayed in Fig. 8, the relevance of other variables can be further concluded. For instance, the effective contraction of each module due to the presence of the neighbor-modules is key to understanding the experimental module contraction, as concluded from analyzing Fig. 6a. The highest value was obtained with a locomotor pattern involving two compressed modules, while the lowest value was with six compressed modules. These experimental values can not only be explained by the effective contraction of individual modules affected by the neighbor modules but also by the bending of the whole Metarpillar due to this contraction having a stiff dorsal silicone surface, as observed in Fig. 6a and 7b. The bending triggered by the buckling-driven module contraction allows a new mechanism to control the friction through a dynamic anchoring between the soft robot and the surface, that is the main mechanism for locomotion in a caterpillar and other crawling organisms [3,38–40,57–58].

All the processes and variables explained above, particularly the dynamic anchoring with the substrate, allowed for our designing of a soft robot based on linear coupling of buckling-driven metamaterial modules, which presents biomimetic locomotion as displayed in Fig. 7b. The principle of the peristaltic locomotion of caterpillars underlies a complex process arising from both antero-posterior and dorso-ventral contractions, which allows for controlling the anchoring with the substrate. This release of friction moves forward with the peristaltic contraction waves, reaching a translation of the body after a gait cycle [39]. This contraction-based locomotion process with dynamic anchoring was successfully mimicked by our buckling-driven Metarpillar by using different locomotion patterns (Fig. 7a). We obtained this dynamic friction control by combining the deformation of the modules (from a square-like to a trapezoid-like shape; Fig. 4c) and the dorsal bending deformation of the Metarpillar (Fig. 7b). As a consequence, our Metarpillar mimics directional migration, generating a limbless locomotor function produced by the coordinate peristaltic contraction wave, even on an isotropic friction surface. Notably, although the caterpillars compress only a limited portion of their bodies at the same time, due to the highly incompressible nature of the internal fluid (haemocoel) (Fig. 1a) [35,38], our Metarpillar presents locomotion even when compressing a large fraction of the body with six modules. This configuration is not observed in nature despite the fact that the number of segments contracted per gait cycle in a caterpillar is variable, for instance, depending on the speed of locomotion [35,37,47]. This result confirms that soft robots are not limited by

the same mechanical constraints and evolutionary trade-offs that organisms face, enabling novel routes of locomotion.

Regarding the speed of our buckling-driven locomotion, Fig. 8 not only shows us the relevance of both the effective contraction of the modules and the bending process but also the friction between the soft robot and surface used. For instance, Fig. 8 displays the empirical locomotion speed of our Metarpillar moving on an isotropic friction paper surface without metal tips and using exclusively the peristaltic contraction of its body for locomotion (Fig. 8: "without anisotropic friction"). This locomotion speed increases with the number of recruited modules in the locomotor pattern when less than three modules are compressed, further presenting values similar to the corrected theoretical speed. However, increasing the number of compressed modules in the locomotion pattern does not cause the speed to significantly increase or even decrease. The reason for this behavior lies in the curvature (bending of the longitudinal axe) of the Metarpillar body when many modules are recruited, pulling back the anterior end when the peristaltic wave begins from the posterior part (Fig. 9). This process produced a slipping backward due to the lack of a proper friction, avoiding a full longitudinal movement and losing locomotor efficiency, and it was observed in locomotor patterns using three modules. It is outstanding that the fractions of contracted modules in our soft robot when this slipping and loss of efficiency are not observed are equivalent to the contracted segment fractions observed in caterpillars. These results suggest that, in addition to the hydrostatic restrictions of the caterpillar, the percentage of body contraction is related to the control of the contact surface with the substrate (in our case with isotropic surface) to avoid losing stability [34–35,37–38].

A different tendency was observed with an anisotropic friction surface, based on a one-direction toothed surface (Fig. 7c), that promotes an effective unidirectional anchor on the substrate, emulating the function of legs and prolegs of the caterpillars to grip the substrate during locomotion. The relevance of an asymmetric friction was recently confirmed in a similar buckling-driven soft robot having locomotion by attachment of two wheels through leg-likes supports. Under asymmetric conditions, unidirectional ratcheting movements was obtained in the soft robot (27). The empirical speeds measured under these conditions confirm the relevance of the surface friction on the efficiency of locomotion (Fig. 8: "anisotropic surface"), as the locomotion speeds of the Metarpillar increased with the modules recruited per locomotor pattern. However, this velocity produced by the locomotion on a translation-promoting toothed surface was lower than both theoretical speeds, although presenting a similar asymptotic tendency. These lower velocities mean that a toothed surface does not completely prevent sliding (skidding) backwards of the ends during locomotion. Notably, by adding two metal tips at the frontal part and two at the rear end of Metarpillar (Fig. 7d), the speed increased significantly (Fig. 8: "anchor and anisotropic surface"). According to previous studies, this is because of the loss of inefficient movements—this system prevents the ends from skidding and, thus, increases locomotion efficiency [48,59–60]. Interestingly, these metal tips that emulate the true legs and prolegs of caterpillars do not seem to intervene negatively in the forward glide. The anisotropic grip is efficient enough for sliding to the front end without loss of energy, and the resulting speeds are as similar as the corrected theoretical speeds. This is to be expected, since the corrected theoretical speed takes into account the real contraction, assuming 100% anisotropy, which is successfully reached with the metal tip ends.

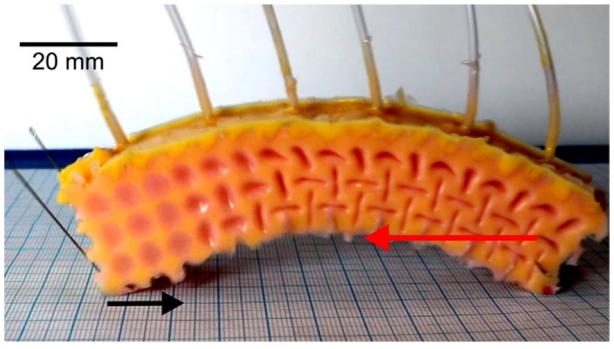

Fig. 9. Picture when 4 modules are recruited. This generates a locomotor conflict when more than two modules are recruited at the same time, without anisotropic grip. The red arrow shows the direction of peristaltic contraction and locomotion; black arrow shows the slip backward of the front part of the Metarpillar. (For interpretation of the references to color in this figure legend, the reader is referred to the web version of this article.)

The Metarpillar not only mimics the locomotion of the caterpillar but also displays an equivalent, or even faster, speed. Considering that a 45 mm caterpillar (*Manduca sexta*) moves at a speed of 3 mm/s [37], we expected a theoretical caterpillar of 120 mm (the length of the Metarpillar) to display a cruising or equivalent speed of 4.9 mm/s with both geometric and dynamic similarities. This equivalent speed was estimated by assuming that both bodies move under the same Froude number (2.04×10^{-5}) [61–62]. The empirical average speed (without anisotropic friction) for our soft robot was found to be 2.2 mm/s and 5.8 mm/s for the locomotor patterns with one contracted module and two contracted modules, respectively (Fig. 7). According to these results, the Metarpillar has dynamic similarity with a caterpillar, using a locomotor pattern having one or two recruited modules, which, as previously discussed, are the locomotor patterns most observed in nature; thus, our soft robot is a very useful kinematic model of a caterpillar (*Manduca sexta*). Fig. 8 further shows that by adding an anisotropic surface, metal tips, and/or changing the locomotor pattern, the Metarpillar can be faster than a caterpillar.

The present study represents the first efforts for using the outstanding properties of auxetic mechanical metamaterials to make biomimetic soft robots. By programing the contraction of buckling-driven modules through locomotive patterns (for instance, with one and two contracted modules), we were able to mimic not only the locomotion of caterpillars but also their dynamic friction and equivalent speeds, representing a novel tool to develop more efficient bio-inspired soft-robots. These findings can be extended to other bioinspired soft robots and devices, and it works for any elastic resin able to present reversible buckling. Indeed, by changing the elastic material the actuation versatility will be as similar as the resin used in this contribution although the pressure needed for the actuation and the velocity of the soft robot will depend on the stiffness of each material tested.

5. Conclusions

Our results showed that the isomorphic characteristic of buckling-driven elastomeric auxetic modules is efficient and can be used to design novel bioinspired soft robots. By serial-coupling these modules, each one independently compressed through a negative air-pressure system, the anterograde peristaltic contraction of the caterpillar crawling can be mimicked. Under defined locomotor patterns (related with the number of modules compressed simultaneously), the soft robot was able to bend in different position of its body resulting in a controlled friction with the surface. The later resulted in a dynamic anchoring process able to bio-mimic the main locomotion mechanism of caterpillars and other crawling organisms. The soft robot speed not only depended on the locomotor pattern and actuation period, but also on the surface-roughness, with improved velocities under a frictional ani-

sotropic surface. Noteworthy, our soft robot presented dynamic similarity with natural caterpillar meaning equivalent velocities. The modular concept used in our Metarpillar soft robot that control independently the compression/deformation of each module, allows to extend the application of this approach to the design of other bioinspired actuation beyond caterpillars.

CRediT authorship contribution statement

B. Grossi: Conceptualization, Methodology, Investigation, Visualization, Funding acquisition, Project administration, Supervision, Writing – original draft, Writing – review & editing. **H. Palza:** Conceptualization, Investigation, Funding acquisition, Project administration, Supervision, Writing – review & editing. **J.C. Zagal:** Conceptualization, Investigation, Visualization, Funding acquisition, Writing – review & editing. **C. Falcón:** Conceptualization, Investigation, Writing – review & editing. **G. During:** Conceptualization, Investigation, Funding acquisition, Writing – review & editing.

Declaration of Competing Interest

The authors declare that they have no known competing financial interests or personal relationships that could have appeared to influence the work reported in this paper.

Acknowledgments

We are thankful to FabLab, University of Chile (www.fablab.uchile.cl), for sharing the facilities to create the required devices for this study.

Funding

This work was funded by ANID – Millennium Science Initiative Program – Code NCN17_092. Chile.

Appendix A. Supplementary data

Supplementary data to this article can be found online at https://doi.org/10.1016/j.matdes.2021.110285.

References

[1] R. Pfeifer, F. Iida, J. Bongard, New robotics: Design principles for intelligent systems, Artif. Life 11 (2005) 99–120.
[2] R. Pfeifer, M. Lungarella, F. Iida, The challenges ahead for bio-inspired 'soft' robotics, Commun. ACM 55 (2012) 76–87.
[3] S. Kim, C. Laschi, B. Trimmer, Soft robotics: A bioinspired evolution in robotics, Trends Biotechnol. 31 (5) (2013) 287–294.
[4] F. Iida, C. Laschi, Soft robotics: Challenges and perspectives, Procedia Comput. Sci. 7 (2011) 99–102.
[5] R. Pfeifer, H. Marques, F. Iida, Soft robotics: the next generation of intelligent machines, in: Twenty-Third International Joint Conference on Artificial Intelligence, China, 2013.
[6] M. Cianchetti, L. Margheri, in: C. Laschi, J. Rossiter, F. Iida (Eds.), Soft Robotics: Trends, Applications and Challenges, Springer, 2017.
[7] J. Rieffel, B. Trimmer, H. Lipson, Mechanism as mind-What tensegrities and caterpillars can teach us about soft robotics, ALIFE (2008) 506–512.
[8] D. Trivedi, C.D. Rahn, W.M. Kier, I.D. Walker, Soft robotics: Biological inspiration, state of the art, and future research, Appl. Bionics Biomech. 5 (3) (2008) 99–117.
[9] F. Ilievski, A.D. Mazzeo, R.F. Shepherd, X. Chen, G.M. Whitesides, Soft robotics for chemists, Angew. Chem. Int. Ed. 50 (8) (2011) 1890–1895.
[10] M.T. Tolley, R.F. Shepherd, B. Mosadegh, K.C. Galloway, M. Wehner, M. Karpelson, R.J. Wood, G.M. Whitesides, A resilient, untethered soft robot, Soft Robot 1 (3) (2014) 213–223.
[11] J. Zou, Y. Lin, C. Ji, H. Yang, A reconfigurable omnidirectional soft robot based on caterpillar locomotion, Soft Robot 5 (2) (2018) 164–174.
[12] D. Agostinelli, F. Alouges, A. DeSimone, Peristaltic waves as optimal gaits in metameric bio-inspired robots, Front. Robot. AI 5 (2018) 99.
[13] A. Rafsanjani, K. Bertoldi, A.R. Studart, Programming soft robots with flexible mechanical metamaterials, Sci. Rob. 4 (2019) eaav7874.
[14] H.-T. Lin, G.G. Leisk, B. Trimmer, GoQBot: A caterpillar-inspired soft-bodied rolling robot, Bioinspirat. Biomimet. 6 (2) (2011) 026007, https://doi.org/10.1088/1748-3182/6/2/026007.
[15] H.T. Lin, D.J. Slate, C.R. Paetsch, A.L. Dorfmann, B.A. Trimmer, Scaling of caterpillar body properties and its biomechanical implications for the use of a hydrostatic skeleton, J. Exp. Biol. 214 (2011) 1194–1204.
[16] S. Seok, C.D. Onal, K.-J. Cho, R.J. Wood, D. Rus, S. Kim, Meshworm: A peristaltic soft robot with antagonistic nickel titanium coil actuators, IEEE/ASME Trans. Mechatron. 18 (5) (2013) 1485–1497.
[17] T. Umedachi, B.A. Trimmer, Design of a 3D-printed soft robot with posture and steering control, in: 2014 IEEE International Conference on Robotics and Automation, 2014, pp. 2874–2879.
[18] M. Rogóż, H. Zeng, C. Xuan, D.S. Wiersma, P. Wasylczyk, Light-driven soft robot mimics caterpillar locomotion in natural scale, Adv. Opt. Mater. 4 (11) (2016) 1689–1694.
[19] A. Rafsanjani, Y. Zhang, B. Liu, S.M. Rubinstein, K. Bertoldi, Kirigami skins make a simple soft actuator crawl, Sci. Rob. 3 (15) (2018), https://doi.org/10.1126/scirobotics.aar7555.
[20] B. Gorissen, D. Melancon, N. Vasios, M. Torbati, K. Bertoldi, Inflatable soft jumper inspired by shell snapping, Sci. Robot. 5 (42) (2020), https://doi.org/10.1126/scirobotics.abb1967.
[21] E. Siéfert, E. Reyssat, J. Bico, B. Roman, Bio-inspired pneumatic shape-morphing elastomers, Nat. Mater. 18 (1) (2019) 24–28.
[22] T. Chen, M. Pauly, P.M. Reis, A reprogrammable mechanical metamaterial with stable memory, Nature 589 (7842) (2021) 386–390.
[23] C. Keplinger, T. Li, R. Baumgartner, Z. Suo, S. Bauer, Harnessing snap-through instability in soft dielectrics to achieve giant voltage-triggered deformation, Soft Matter 8 (2) (2012) 285–288.
[24] D. Yang, B. Mosadegh, A. Ainla, B. Lee, F. Khashai, Z. Suo, K. Bertoldi, G.M. Whitesides, Buckling of elastomeric beams enables actuation of soft machines, Adv. Mater. 27 (41) (2015) 6323–6327.
[25] D. Yang, M.S. Verma, J.-H. So, B. Mosadegh, C. Keplinger, B. Lee, F. Khashai, E. Lossner, Z. Suo, G.M. Whitesides, Buckling pneumatic linear actuators inspired by muscle, Adv. Mater. Technol. 1 (3) (2016) 1600055, https://doi.org/10.1002/admt.201600055.
[26] T. Chen, O.R. Bilal, K. Shea, C. Daraio, Harnessing bistability for directional propulsion of soft, untethered robots, Proc. Natl. Acad. Sci. 115 (22) (2018) 5698–5702.
[27] G. Wang, M. Li, J. Zhou, Modeling soft machines driven by buckling actuators, Int. J. Mech. Sci. 157-158 (2019) 662–667.
[28] J.T.B. Overvelde, S. Shan, K. Bertoldi, Compaction through buckling in 2D periodic, soft and porous structures: effect of pore shape, Adv. Mater. 24 (17) (2012) 2337–2342.
[29] K. Bertoldi, P.M. Reis, S. Willshaw, T. Mullin, Negative Poisson's ratio behavior induced by an elastic instability, Adv. Mater. 22 (3) (2010) 361–366.
[30] S. Janbaz, F.S.L. Bobbert, M.J. Mirzaali, A.A. Zadpoor, Ultra-programmable buckling-driven soft cellular mechanisms, Mater. Horiz. 6 (6) (2019) 1138–1147.
[31] J. Bishop-Moser, G. Krishnan, C. Kim, S. Kota, Design of soft robotic actuators using fluid-filled fiber-reinforced elastomeric enclosures in parallel combinations, in: 2012 IEEE/RSJ International Conference on Intelligent Robots and Systems, 2012, pp. 4264–4269.
[32] H.T. Lin, B. Trimmer, The substrate as a skeleton: ground reaction forces from a soft-bodied legged animal, J. Exp. Biol. 213 (2010) 1133–1142.
[33] B.A. Trimmer, H.-t. Lin, Bone-free: Soft mechanics for adaptive locomotion, Integr. Comp. Biol. 54 (6) (2014) 1122–1135.
[34] J. Brackenbury, Caterpillar kinematics, Nature 390 (1997) 453.
[35] J. Brackenbury, Fast locomotion in caterpillars, J. Insect Physiol. 45 (1999) 525–533.
[36] A.G. Mark, S. Palagi, T. Qiu, P. Fischer, Auxetic metamaterial simplifies soft robot design, in: 2016 IEEE International Conference on Robotics and Automation (ICRA), 2016, pp. 4951–4956.
[37] L.I. Van Griethuijsen, B.A. Trimmer, Kinematics of horizontal and vertical caterpillar crawling, J. Exp. Biol. 212 (2009) 1455–1462.
[38] L.I. van Griethuijsen, B.A. Trimmer, Locomotion in caterpillars, Biol. Rev. 89 (3) (2014) 656–670.
[39] Y. Tanaka, K. Ito, T. Nakagaki, R. Kobayashi, Mechanics of peristaltic locomotion and role of anchoring, J. R. Soc. Interface 9 (67) (2012) 222–233.
[40] H. Fang, Y. Zhang, K.W. Wang, Origami-based earthworm-like locomotion robots, Bioinspirat. Biomimet. 12 (6) (2017) 065003, https://doi.org/10.1088/1748-3190/aa8448.
[41] W. Wu, W. Hu, G. Qian, H. Liao, X. Xu, F. Berto, Mechanical design and multifunctional applications of chiral mechanical metamaterials: A review, Mater. Des. 180 (2019) 107950.
[42] A.L. Wickeler, H.E. Naguib, Novel origami-inspired metamaterials: Design, mechanical testing and finite element modelling, Mater. Des. 186 (2020) 108242.
[43] N.C. Paxton, R. Daley, D.P. Forrestal, M.C. Allenby, M.A. Woodruff, Auxetic tubular scaffolds via melt electrowriting, Mater. Des. 193 (2020) 108787.
[44] J.M. Hur, D.S. Seo, K. Kim, J.K. Lee, K.J. Lee, Y.Y. Kim, D.N. Kim, Harnessing distinct deformation modes of auxetic patterns for stiffness design of tubular structures, Mater. Des. 198 (2021) 109376.

[45] A. Rafsanjani, Y. Zhang, B. Liu, S.M. Rubinstein, K. Bertoldi, Kirigami skins make a simple soft actuator crawl, Sci. Rob. 3 (15) (2018), https://doi.org/10.1126/scirobotics.aar7555.
[46] G.M. Hughes, P.J. Mill, Locomotion: Terrestrial, in: The Physiology of Insecta, Academic Press, 1974, pp. 335–379.
[47] W.A. Woods, S.J. Fusillo, B.A. Trimmer, Dynamic properties of a locomotory muscle of the tobacco hornworm Manduca sexta during strain cycling and simulated natural crawling, J. Exp. Biol. 211 (2008) 873–882.
[48] A.A. Calderón, J.C. Ugalde, L. Chang, J.C. Zagal, N.O. Pérez-Arancibia, An earthworm-inspired soft robot with perceptive artificial, Bioinspirat. Biomimet. 14 (2019) 056012.
[49] E.W. Hawkes, C. Majidi, M.T. Tolley, Hard questions for soft robotics, Sci. Robot. 6 (2021) eabg6049.
[50] K. Bertoldi, V. Vitelli, J. Christensen, M. van Hecke, Flexible mechanical metamaterials, Nat. Rev. Mater. 2 (11) (2017), https://doi.org/10.1038/natrevmats.2017.66.
[51] S. Babaee, J. Shim, J.C. Weaver, E.R. Chen, N. Patel, K. Bertoldi, 3D soft metamaterials with negative Poisson's ratio, Adv. Mater. 25 (36) (2013) 5044–5049.
[52] J. Shim, S. Shan, A. Košmrlj, S.H. Kang, E.R. Chen, J.C. Weaver, K. Bertoldi, Harnessing instabilities for design of soft reconfigurable auxetic/chiral materials, Soft Matter 9 (34) (2013) 8198, https://doi.org/10.1039/c3sm51148k.
[53] N. Hu, R. Burgueño, Buckling-induced smart applications: Recent advances and trends, Smart Mater. Struct. 24 (6) (2015) 063001, https://doi.org/10.1088/0964-1726/24/6/063001.
[54] T. Mullin, S. Willshaw, F. Box, Pattern switching in soft cellular solids under compression, Soft Matter 9 (20) (2013) 4951, https://doi.org/10.1039/c3sm27677e.
[55] P.A.L.S. Martins, R.M. Natal Jorge, A.J.M. Ferreira, A comparative study of several material models for prediction of hyperelastic properties: Application to silicone-rubber and soft tissues, Strain 42 (2006) 135–147.
[56] R.M. Alexander, Principles of Animal Locomotion, Princeton University Press, 2003.
[57] H.Y. Elder, Direct peristaltic progression and the functional significance of the dermal connective tissues during burrowing in the polychaete Polyphysia crassa (Oersted), J. Exp. Biol. 58 (1973) 637–655.
[58] H. Marvi, J. Bridges, D.L. Hu, Snakes mimic earthworms: Propulsion using rectilinear travelling waves, J. R. Soc. Interface 10 (84) (2013) 20130188, https://doi.org/10.1098/rsif.2013.0188.
[59] C.D. Onal, R.J. Wood, D. Rus, An origami-inspired approach to worm robots, IEEE/ASME Trans. Mechatron. 18 (2012) 430–438.
[60] J. Tuo, H. Zang, Y. Shu, D. Liu, N. Zhu, B. Liao, T. Zhou, Q. Wang, A peristaltic bionic robot controlled by a single elastic-gasbag, in: 2018 WRC Symposium on Advanced Robotics and Automation (WRC SARA), 2018, pp. 249–254.
[61] R.M. Alexander, Estimates of speeds of dinosaurs, Nature 261 (1976) 129–130.
[62] B. Grossi, M. Canals, Comparison of the morphology of the limbs of juvenile and adult horses (Equus caballus) and their implications on the locomotor biomechanics, J. Exp. Zool. Part A: Ecol. Genet. Physiol. 313 (2010) 292–300.